

Controllable harmonic mode locking and multiple pulsing in a Ti:sapphire laser

Xiaohong Han, Jian Wu, and Heping Zeng*

State Key Laboratory of Precision Spectroscopy, and Department of Physics, East China Normal University, Shanghai 200062, China

*Corresponding author: hpzeng@phy.ecnu.edu.cn

Abstract: A new way to control the harmonic mode-locking and multiple pulsing operation with the pulse duration unaffected of a Kerr-lens mode-locked Ti:sapphire laser was demonstrated. When the effective nonlinear length of the nonlinear medium which was inserted in the Ti:sapphire laser was varied by changing the position of the medium or the pump power of the laser, stable harmonic mode-locking and multiple-pulse operation were observed.

©2008 Optical Society of America

OCIS codes: (140.0140) Lasers and laser optics; (140.4050) Mode-locked lasers (190.7110) Ultrafast nonlinear optics; (260.2030) Dispersion; (320.5520) Pulse compression.

References and links

1. P. Grelu, F. Belhache, F. Gутty, and J. M. Soto-Crespo, "Relative phase locking of pulses in a passively mode-locked fiber laser," *J. Opt. Soc. Am. B* **20**, 863 (2003).
2. Ph. Grelu and J. M. Soto-Crespo, "Multisoliton states and pulse fragmentation in a passively mode-locked fibre laser," *J. Opt. B: Quantum Semiclassical Opt.* **6**, S271 (2004).
3. A. Komarov, H. Leblond, and F. Sanchez, "Multistability and hysteresis phenomena in passively mode-locked fiber lasers," *Phys. Rev. A* **71**, 053809 (2005).
4. J. Aus der Au, D. Kopf, F. Morier-Genoud, M. Moser, and U. Keller, "60-fs pulses from a diode-pumped Nd:glass laser," *Opt. Lett.* **22**, 307 (1997).
5. M. J. Lederer, B. Luther-Davies, H. H. Tan, C. Jagadish, N. N. Akhmediev, and J. M. Soto-Crespo, "Multipulse operation of a Ti:sapphire laser mode locked by an ion-implanted semiconductor saturable-absorber mirror," *J. Opt. Soc. Am. B* **16**, 895 (1999).
6. C. Spielmann, P. F. Curley, T. Brabec, and F. Krausz, "Ultrabroadband femtosecond lasers," *IEEE J. Quantum Electron.* **30**, 1100 (1994).
7. C. Wang, W. Zhang, K. F. Lee, and K. M. Yoo, "Pulse splitting in a self-mode-locked Ti: sapphire laser," *Opt. Commun.* **137**, 89 (1997).
8. B. C. Collings, K. Bergman, and W. H. Knox, "True fundamental solitons in a passively mode-locked short-cavity Cr⁴⁺:YAG laser," *Opt. Lett.* **22**, 1098 (1997).
9. J. H. Lin, W. F. Hsieh, and H. H. Wu, "Harmonic mode locking and multiple pulsing in a soft-aperture Kerr-lens mode-locked Ti:sapphire laser," *Opt. Commun.* **212**, 149 (2002).
10. B. C. Collings, K. Bergman, and W. H. Knox, "Stable multigigahertz pulse-train formation in a short-cavity passively harmonic mode-locked erbium/ytterbium fiber laser," *Opt. Lett.* **23**, 123 (1998).
11. D. Y. Tang, L. M. Zhao, B. Zhao, and A. Q. Liu, "Mechanism of multisoliton formation and soliton energy quantization in passively mode-locked fiber lasers," *Phys. Rev. A* **72**, 043816 (2005).
12. J. Nathan Kutz, B. C. Collings, K. Bergman, and W. H. Knox, "Stabilized pulse spacing in soliton lasers due to gain depletion and recovery," *IEEE J. Quantum Electron.* **34**, 1749 (1998).
13. C. J. Zhu, J. F. He, and S. C. Wang, "Generation of synchronized femtosecond and picosecond pulses in a dual-wavelength femtosecond Ti:sapphire laser," *Opt. Lett.* **30**, 561 (2005).

1. Introduction

As an effective way to generate high repetition rate pulsed laser sources, multi-pulse operation based harmonic mode-locking has drawn much attention in both bulk and fiber lasers [1-7]. It was found that third-order harmonic mode-locking pulses could be constructed in a passively mode-locked Cr⁴⁺:YAG laser [8], and fourth-order harmonic mode-locking pulses were observed in a Kerr-lens mode-locked (KLM) Ti:sapphire laser [9]. With apropos intra-cavity power, up to 11 pulses were obtained in a passively mode-locked erbium/ytterbium fiber laser

[10]. Multi-pulse operation with femtosecond (fs) pulse spacing limited by the pulse duration in an KLM Ti:sapphire laser was reported [7]. Theoretically, Ginzburg-Landau equation taking account of the effect of a bandpass filter was used to simulate the pulse-splitting of a mode-locked Ti:sapphire laser started with a semiconductor saturable-absorber mirror [5]. Peak-power-limiting effect was proved to be responsible for multi-soliton generation in a passively mode-locked fiber laser [11], and the gain depletion and recovery dynamics in the gain medium was successfully used in understanding different pulse spacings in soliton lasers [12]. Here, we performed a further study on the influence of the Kerr effect on multi-pulse operation of the KLM ultrashort lasers, which would be essential for such kind of lasers.

In this paper, we experimentally demonstrate that harmonic mode-locking and multi-pulse operation in a KLM Ti:sapphire laser can be controlled by varying the intra-cavity Kerr effect, which is performed by tuning the position of an inserted nonlinear crystal or changing the pump intensity. Moreover, for a stable multi-pulse operation, the value of the intra-cavity net negative dispersion is limited by the Kerr effect. These results allow us a better understanding of the multi-pulse operation of the KLM laser and provide a possible way to control it.

2. Experiment and results

A schematic of the Ti:sapphire laser used in our experiment is shown in Fig. 1. It contains two Brewster-cut Ti:sapphire crystals (Ti:S1 and Ti:S2) in two confocal cavities, and Ti:S1 (2.5-mm-thick) is used as the gain medium for the laser while Ti:S2 (5-mm-thick) is used as a nonlinear medium. Three pairs of broadband high-reflection (HR) chirped mirrors (M1-M2, M3-M4, and M5-M6), each with an average group velocity dispersion (GVD) of -70 fs^2 , are used to compensate for the positive intra-cavity GVD. M1, M2, M5, and M6 are concave mirrors with the same radius of 100 mm, and a 3% output coupler (OC) is used. A pair of fused silica prism (P1 and P2) with a separation of 397 mm is inserted in the cavity for additional tunability of the intra-cavity GVD. The total cavity length is about 1875 mm, which corresponds to a round-trip time of 12.5 ns. A commercial autocorrelator and a power meter are used to measure the pulse duration and the average output power, respectively. A sampling oscilloscope and an rf-spectrum analyzer are used to monitor the pulse evolution and its corresponding power-spectrum with the help of a high-speed detector.

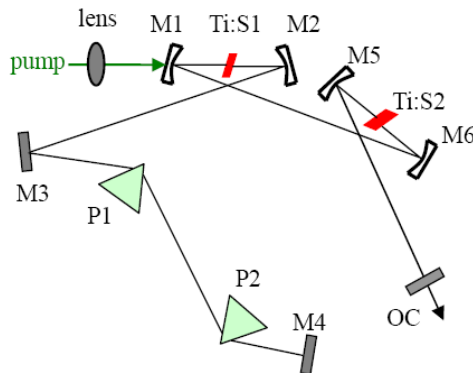


Fig. 1. Schematic of the Ti:Sapphire laser. Ti:S1 and Ti:S2 are two Ti:sapphire crystals with 2.5 mm and 5 mm thickness, respectively. M1-M6 are broadband HR coated chirped mirrors and OC is the output coupler. M1, M2, M5 and M6 are concave mirrors with a curvature radius of 100 mm. The fused silica prisms P1 and P2 supply tunable dispersion.

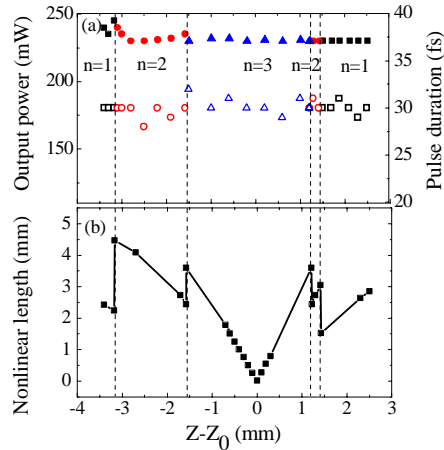


Fig. 2. (a) The average output power (solid symbol) and the pulse duration (open symbol) as functions of the position of Ti:S2 relative to the focus of the confocal cavity, where z is the position of Ti:S2 while z_0 is the position of the focus, and n is the number of pulses in a round-trip time. (b) The effective nonlinear length as a function of the position.

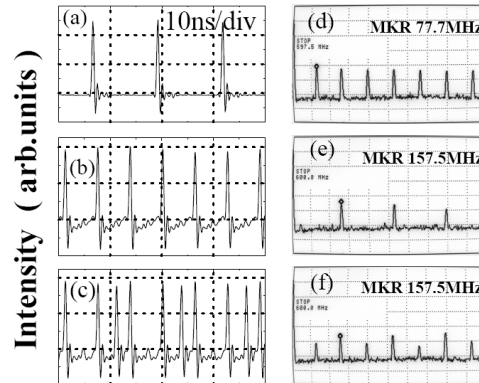


Fig. 3. Pulse trains and the corresponding rf-spectra observed while varying the position of Ti:S2. Normal mode locking (a and d), second harmonic mode-locking (b and e), and triple-pulse operation (c and f) are observed.

Mode-locking can be achieved readily by pushing one of the prisms quickly as M2 is tuned to a suitable position. The position of the nonlinear crystal Ti:S2 can be tuned continuously in a precise way. While translating Ti:S2 inside the laser cavity, the output average power and pulse duration experience no observable changes. Figure 2(a) shows the output power, the pulse duration and the number of the pulses observed in a cavity round-trip time as functions of the position of Ti:S2 relative to the focus of the confocal cavity. Five regions can be found in the figure with different number (n) of pulses in a round-trip time. It shows a strong tendency that the closer the Ti:S2 to the focus, the more pulses are observed. The asymmetry of Fig. 2 with respect to $Z-Z_0$ is caused by the asymmetry of the beam waist in the cavity. The pulse train and the corresponding power spectrum are shown in Fig. 3. At certain positions, stable second-order harmonic mode-locking is found and three pulses with unequal nanosecond interpulse spacing are observed. Once the multiple pulses are structured, the harmonic mode-locking where all pulses have an equal interpulse spacing can be well explained by the transient gain depletion and recovery mechanism [12]. Since the gain

recovery time of Ti:sapphire is much longer than the round-trip time, if the n ($n \geq 2$) pulses in the cavity have an unequal separation, the gain for each pulse will be different. So does the group velocity. Under this situation, after a large number of round trip in the cavity, a stable state of harmonic mode-locking is structured. The timing jitter of a Gaussian pulse can be given by $t_j = \tau_{XC} - \tau_{AC}$, where τ_{XC} and τ_{AC} are the full-width at half-maximums (FWHM) of the cross- and auto-correlation of the laser output pulses, respectively [13]. As shown in Fig. 4(a), the auto- and cross-correlation are measured with a home-made correlator for the second harmonic mode-locked laser pulses. A 0.2-mm-thick beta barium borate crystal is used for the sum-frequency generation of two cross-overlapped pulses, and an avalanche photodiode is used for the detection. In the cross-correlation measurement, the time delay is adjusted around 6.125 ns for two adjacent harmonic pulses. The auto- and cross-correlation FWHMs are 40 and 45 fs, indicating a pulse-to-pulse timing jitter of 5 fs for the adjacent harmonic pulses. Meanwhile from the RF spectrum shown in Fig. 4(b), we can find that the cavity fundamental suppression (super-mode suppression) is better than 38 dB.

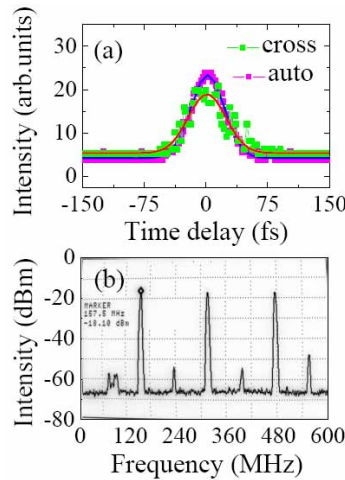


Fig. 4. (a). Cross-correlation (green line and symbol) and auto-correlation (magenta line and symbol) measurements when the laser is second harmonic mode-locked. The blue (red) line is the Gaussian simulation of the cross-correlation (auto-correlation) trace. (b) For the second harmonic mode-locking, the RF spectrum shows a super-mode suppression >38 dB.

3. Analysis

The dependence of the multi-pulse operation on the position of the nonlinear crystal can be understood as follows. The pulse propagation in the cavity can be described by the nonlinear Schrödinger equation:

$$i \frac{\partial u}{\partial z} + \frac{\beta_2}{2} \frac{\partial^2 u}{\partial t^2} + \gamma |u|^2 u = 0, \quad (1)$$

where u is the electric field envelop, and β_2 is the net intra-cavity GVD. The nonlinear coupling term corresponds to Kerr effect with the coefficient $\gamma = 2n_2 / (\lambda \omega^2)$, where n_2 is the nonlinear refraction index of Ti:sapphire, λ is the central wavelength of the carrier envelope, and ω is the beam waist. Obviously, as the crystal moves towards to the focus, the beam waist becomes smaller and the Kerr effect becomes stronger. As there are no visible

changes of β_2 (see Fig. 2), an intuitional conclusion can be derived that the action of Kerr effect in the crystal should be responsible for the pulse splitting. To be more precise and to reveal the underlying physical mechanism, we take into account the combined effects of Kerr nonlinearity and positive GVD in the medium and also the negative GVD inside the laser cavity. At first, to describe the pulse evolution along the medium, we use a parameter $N = L_D / L_{NL}$ to characterize the dispersion effect over Kerr nonlinearity, where L_D is the dispersion length related to the pulse duration (T_0) and GVD (β) in the medium in the form of $L_D = T_0^2 / |\beta|$, while L_{NL} is the effective nonlinear length related to the peak power P and γ in the form of $L_{NL} = 1 / (\gamma P)$. In our experiment, with $T_0 = 30$ fs, $\beta = 580$ fs²/cm, $P = 3.3 \times 10^6$ W with the output power around 230 mW, and $\gamma = 7.5 \times 10^{-4}$ (W·m)⁻¹ with $\omega \approx 10$ μ m, we get $N = 36.8$, which means that the Kerr effect plays a dominant role on the pulse evolution along the medium in comparison with the dispersion effect. The Kerr nonlinearities may function as self-phase modulation (SPM) and four-wave mixing between different frequency modes in the frequency domain, self-focusing of the laser beam in the space domain, or self pulse steepening in the time domain. In any cases, the nonlinear interaction can well-described by the nonlinear term in Eq. (1). The self-focusing results in changes of the beam waist and accordingly the peak power, which is comparably small than those caused by the translation of the Ti:S2 crystal. We thus neglect the spatial changes in our analysis and focus on the pulse changes in the time (frequency) domain for the sake of simplicity. SPM actually plays a dominant role on pulse splitting among all the mentioned Kerr nonlinearities. Four-wave mixing among different frequency modes broadens the pulse spectra and is equivalent to SPM in the frequency domain. Then, taking the intra-cavity net negative GVD into account, the pulse splitting mechanism can be shown as side-lobe pulse generation [7]. Since the SPM provides positive linear frequency chirp at the center of the pulse and negative nonlinear chirp at the edges, when the pulse passes through the prism pair, it splits into three pulses because of the action of negative GVD. But only the two pulses formed from the edges can be sustained and grow into stable double pulses while the pulse from the center with much less energy will disappear. As N is much larger than one in our laser, it is impossible for the central pulse getting enough energy to be sustained, which is different from Ref. [7]. The three-pulse operation here can be explained as the reaction of the pulse splitting operation shown above. Since the two pulses sustained in the cavity can carry different energy, it is comprehensible that the stronger one can split again with the increasing effect of SPM and then stable three pulses can be obtained. Figure 5 shows the dependence of the pulse evolution on the value of N . The arrows show the pulse evolution while Ti:S2 is translated hereabout the focus orderly. When N is large enough, the pulse in the cavity develops into two pulses suddenly, meanwhile the value of N decreases to the half level because of the intra-cavity energy redistribution. As N keeps on increasing, the two pulses develop into three pulses. The maximum of N appears when Ti:S2 is in the confocal focus. If we keep on translating Ti:S2, N decreases. So does the number of pulses in a round-trip time. Since the dispersion length of the medium keeps constant, the dependence of pulse splitting on the effective nonlinear length related to the Kerr effect is shown clearly. The evolution of the effective nonlinear length while Ti:S2 is translated can be found in Fig. 2(b).

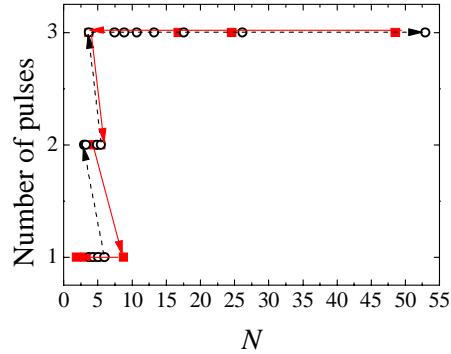


Fig. 5. The dependence of the number of pulses in a round-trip time on the value of N . The arrows show the pulse evolution while Ti:S2 is translated hereabout the confocal focus orderly. Here dash line and circle correspond to the situation that Ti:S2 moves towards the focus while solid line and square correspond to the opposite.

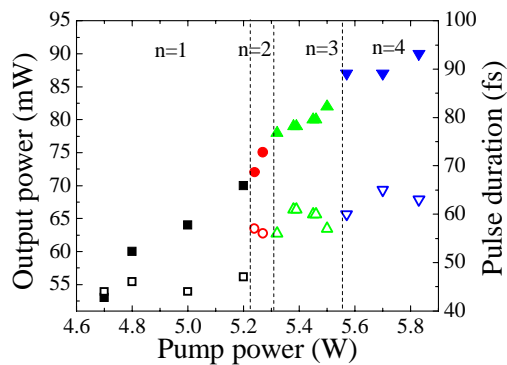


Fig. 6. The average output power (solid symbol) and the pulse duration (open symbol) as functions of the pump power, where n is the number of pulses in a round-trip time.

Two more experiments are performed to validate the Kerr effect dominant mechanism. Harmonic mode-locking and multiple pulses are found while the pump power or negative GVD is changed. Figure 6 gives the output power, the pulse duration and the number of the pulses observed in a round-trip time as a function of pump power. Depending on the value of n , four regions appear in the figure. While the pump power increases, the peak power inside the crystal increases, which enhances the Kerr effect. So it is not difficult to understand that at certain levels, the side-lobe pulses are generated. Furthermore, when the pump power is above a critical value, the stable mode-locking mechanism is destroyed and a continuous-wave component are found on the spectrum. The number of pulses in a cavity round-trip time decreases while the continuous-wave component increases, which shows the dependence of the pulse splitting on the Kerr effect.

It's not surprising that multi-pulse operation exists in a laser cavity when the intra-cavity negative GVD is decreased below a critical value. According to previous reports [5,9], in the

presence of mere negative intra-cavity GVD, the lower the value of $|\beta_2|$ the more pulses could be found. But our experiment results show that pulse splitting happens only when the negative GVD is limited in a certain range. As the negative GVD is varied by changing the insertion width of the second prism P2, stable mode-locking in the cavity develops into multi-pulse operation firstly and then returns to stable mode-locking with single pulse in a round-trip time at a critical value as the GVD keeps decreasing. Figure 7 shows this tendency clearly. It also shows the output power and pulse duration as functions of the negative GVD. Using the mechanism discussed above, we can find out that the requirement of a certain amount of the GVD is due to the decreasing Kerr effect in the medium caused by the decreasing peak power. When the Kerr effect is below the critical level or even less than the positive GVD, the side-lobe pulse generation can't occur and only stable mode-locking with one pulse can be observed in a round-trip time.

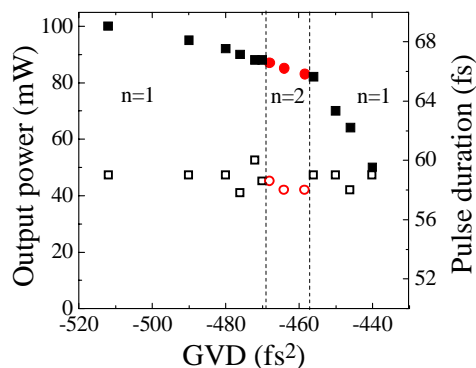


Fig. 7. The average output power (solid symbol) and pulse duration (open symbol) as functions of the net negative intra-cavity GVD where n is the number of pulses.

4. Conclusion

In summary, we demonstrate a new way to control harmonic mode-locking and multi-pulse operation of a KLM Ti:sapphire laser. As the effective nonlinear length of the medium intra-cavity is varied by adjusting the position of the medium or the pump power of the laser, pulse splitting and harmonic mode-locking are observed. A limitation of the net negative GVD caused by the change of the effective nonlinear length is found. These results are explained well by side-lobe pulse generation and transient gain depletion and recovery.

Acknowledgments

This work was partly supported by National Natural Science Fund (10525416 & 10774045), National Key Project for Basic Research (2006CB806005), Program for Changjiang Scholars and Innovative Research Team, Shanghai Science and Technology Commission (06SR07102 & 06JC14025), and Shanghai leading Academic Discipline project (B408).